Wasit Journal of Engineering Sciences
Journal homepage: https://ejuow.uowasit.edu.iq
Vol. 14 No. 3 September 2026, pp.120-137
https://doi.org/10.31185/ejuow.v14i3.924

ISSN 2305-6932
Original Research

Seismic Performance Evaluation of Mid-Rise RC Buildings Considering Soil-Structure Interaction and Different Foundations Rigidities

Issa Al-Musawi [1], Asad H. Aldefae [1], Karrar Al-Lami [1], K.I.M Ismail [2]

[1] Department of Civil Engineering, College of Engineering, Wasit University, Wasit, Iraq.

[2] Civil and Environmental Engineering Department, The Hong Kong University of Science and Technology, Hong Kong SAR

Corresponding Author Email: almu20sawi@gmail.com

Received Mar.25, 2024	Revised Aug.19, 2025	Accepted Aug.22, 2025	Online Sep.1, 2026

ABSTRACT

This study evaluates the seismic performance of an existing seven-story reinforced concrete parking garage (85 m × 50 m plan) that was not originally designed for seismic loads. The structure, featuring flat slabs, ordinary shear walls, and a circular vehicular ramp, is currently supported on bearing piles. Three-dimensional finite-element time-history analyses were conducted in Plaxis 3D using the local Halabja 2017 Mw 7.3 acceleration record. Parametric investigations compared the existing pile system against alternative raft foundations with plan dimensions of 1.1B, 1.5B, and 2B, where B = 50 m on both the actual four-layer site soil and an idealized soft-soil profile; a fourteen-story variant was also analyzed to examine height effects. Results show that the 14-story model on soft soil with the smallest raft (1.1B) exhibited the most critical response: roof displacement reached 26.5 cm, inter-storey drift peaked at 1.61 %, and the fundamental period lengthened to 2.46 s. Conversely, increasing the raft size to 2B reduced displacement and drift toward the fixed-base values (e.g., 7-storey site-soil displacement dropped from 7.0 cm.at 1.1B to 6.8 cm at 2B versus 6.5 cm fixed-base). Base shear followed an inverse trend, decreasing with soil flexibility but recovering toward the fixed-base level as raft stiffness increased. It is recommended that raft foundations be sized at least 1.5B–2B for mid-rise RC structures on deformable soils to limit SSI-induced period lengthening and drift amplification; explicit 3D SSI analysis should be mandated for seismic assessment of existing non-seismic buildings in seismically active regions such as Iraq.

Keywords: SSI, Seismic Performance, Raft Foundation, Finite Element Analysis, Mid-Rise Building

1. Introduction

Soil–structure interaction (SSI) is an interdisciplinary field which involves structural and geotechnical engineering [1]. The dynamic response of a structure depends on the properties of underlying soil, structure, and nature of excitation. The process in which the response of the soil influences the motion of the structure and vice versa is referred to as SSI [2]. The conventional non-interaction analysis of buildings without considering the influence of the soil may result in overestimation or underestimation of the structural response. Hence, soil–structure interaction is therefore crucial for assessing the seismic hazards and designing more resilient structures for potential high-intensity earthquake scenarios at seismically active regions [1,2]. For structures founded on rock, the extremely high stiffness of the rock constrains the rock motion, and the structural response is regarded to be the same as that of a fixed-base structure during ground motion. The same structure responds differently when supported on soft soil. The motion of the base of the structure diverges from the free-field motion due to the incompetence of the foundation to adapt to the deformations of the free field. Besides, the dynamic response of the structure induces deformation of the supporting soil. The response of the soil regulates the motion of the structure, and the response of the structure regulates the motion of the soil [1,2].

Accordingly, this study evaluates the seismic performance of an existing mid-rise reinforced-concrete parking structure that was not originally designed for seismic actions. The response is assessed for different foundation systems and soil conditions to quantify the influence of soil–structure interaction and to identify configurations that provide improved seismic performance.

1.1 Problem Statement and Study Objectives

The seismic response of mid-rise reinforced concrete structures is influenced by parameters such as lateral displacement, interstory drift, natural period, and base shear. In this study, the historic Halabja 2017 earthquake record in the Y-Y direction was applied at the base of the model as bedrock ground motion. The effects of soil–structure interaction were investigated by comparing a fixed-base reference model and the existing bearing-pile foundation with alternative raft foundations having plan dimensions of 1.1.1B, 1.5B, and 2B, where B is the 50 m reference building width. Two types of soil were considered: the actual four-layer site profile and an idealized soft soil model to reflect more deformable ground conditions.

Structural configurations included buildings of 7 and 14 stories, both with footprints of 85 by 50 meters and floor heights of 3.25 meters, except for the ground floor, which was set at 4.50 meters. The reinforced concrete was modeled with a compressive strength of 55 MPa. Finite element simulations were carried out using Plaxis 3D, where all slab-to-beam and beam-to-column connections were assumed to be fully fixed. The responses of the coupled systems were compared to the fixed-base case to assess how soil type, foundation design, and building height influence the dynamic performance of RC structures. Therefore, this study aims to evaluate the effect of the number of stories on the seismic response of a reinforced concrete parking structure under fixed-base conditions and to assess the impact of soil–structure interaction on seismic behavior for different soil types and raft foundation sizes.

2. Related Work

2.1 Previous SSI Studies

When the supporting medium of soil is considered in the analysis, the dynamic characteristics of the structural system get altered when compared to those with the conventional completely restrained supports, as soil forms the constitutional part of the structure. At the beginning, SSI has been viewed as beneficial during seismic motion, but changing research trends have resulted in different notions about the phenomenon [1]. Despite the fact that SSI increases damping, which is beneficial, it also causes additional displacement to the overall structure, which has detrimental effects. Gazetas and Mylonakis [1] noticed that the supporting soil medium allows certain movements due to its natural flexibility, which decreases the overall stiffness of the structural system and increases the natural periods of the system. The study also highlighted the influence of partial fixity of structures at the foundation level due to soil flexibility altering the response. Studies carried out by Stewart et al. [2], Gazetas and Mylonakis [1] state that SSI can be detrimental, and neglecting its influence could lead to uncertainties in both the superstructure and foundations design, especially for structures on soft soil deposits. Balendra and Heidebrecht [3] and Ghannam et al. [4] demonstrated the significance of SSI effects in medium and long- period structures. Recorded earthquake spectra indicate that SSI turns out to be a significant factor for the maximum acceleration occurring at a period greater than 1.0 s. The structure fundamental period tends to be longer with considering SSI that increases the dynamic response that may not match with the conventional design code. Studies of the Bucharest earthquake 1977, Mexico earthquake 1985, and Kobe earthquake 1995 showed an increase in the seismic response of structures despite a possible increase in damping, as reported by Gazetas and Mylonakis [1]. This study reported that the Mexico earthquake was particularly destructive to 10–12 storey unbraced buildings founded on soft clay, for which the period increased from about 1.0 s (as per conventional fixed-base assumption) to nearly 2.0 s due to SSI. A comprehensive study including SSI effects carried out by Stewart et al. [2] for 77 strong-motion datasets at 57 actual building sites that cover a wide range of structural and geotechnical conditions revealed that inertial SSI effects can be conveyed by a fundamental natural period lengthening ratio and foundation damping factor. Accordingly, the fundamental natural period of the overall system and total damping are increased by considering SSI effects. The effect of SSI in increasing the lateral deflections and corresponding inter-storey drifts of the structure, pushing the structure to behave in the inelastic range, resulting in severe damage of the structure was studied by Alavi and Krawinkler [6], Adam et al. [7], Galal and Naimi [8], and Stewart et al. [9] However, seismic response generally decreases due to the influence of SSI for medium- to high-rise buildings. Considerable variation in lateral natural periods and base shear were found, signifying the need of incorporating the effect of SSI in the seismic analysis of buildings. The effect of SSI on stress resultants experienced by the raft and the interface between the rock and raft of massive concrete structures supported over a raft foundation was carried out by Rajasankar et al. [5].

Relevant research [10] assessed the seismic behavior of 15-storey medium-rise structures with plan dimensions of 15 × 15 m, a total height of 45 m, and a frame system supported on a raft foundation. Soil-structure interaction was simulated using Plaxis 3D software, with soil stiffness characterized by elasticity parameters. Multiple time-history analyses were conducted with varying raft dimensions (1.3B, 1.5B, and 2.0B), where B denotes the building width of 15 m, alongside different column sizes. The model incorporating silty sand soil was compared to a fixed-base case. Results demonstrated that for raft sizes 1.5B and 2.0B, increased column dimensions reduced lateral deflections, while larger columns and rafts amplified base shear across all configurations. Additionally, larger raft dimensions combined with reduced column sizes minimized foundation rotation angles. The study concluded that optimization of both column and raft dimensions is essential for structural stability, and increased raft sizes effectively mitigate foundation rocking. In complementary research [1], the seismic performance of a six-storey, four-bay wall-frame structure on pile foundations was evaluated. Multiple two-layered soil deposits were examined by varying layer thicknesses and properties. Findings revealed that soil-structure interaction increased global lateral flexibility. Fixed-base models exhibited significantly higher horizontal displacements, impacting seismic gap requirements, while SSI models showed prolonged fundamental periods and reduced base shear compared to fixed-base counterparts. Structural displacements increased under SSI conditions but remained nearly constant for fixed-base cases.

2.2 Seismicity and Historical Earthquakes in Iraq

Iraq lies at the northeastern margin of the Arabian Plate (fig. 1) adjacent to the Zagros–Taurus tectonic belts, where convergence with the Iranian and Anatolian plates results in active crustal deformation and recurring seismicity [12,13]. Historical records confirm that earthquakes have repeatedly affected northern and northeastern Iraq, particularly along the Iraq–Iran border zone. An earthquake catalogue for Iraq covering the period 1900–1988 was reported to contain 1,030 events with magnitudes ranging between 3.7 to 7.4 on the Richter scale [12]. In addition, a homogeneous magnitude catalogue spanning 1900–2010 was developed using a unified moment magnitude scale (Mw), providing an updated basis for seismicity characterization and completeness assessment [17]. Table 1 summarizes notable earthquakes in Iraq from 820 to 2018, illustrating the recurrence of damaging events. Collectively, these datasets and recent probabilistic seismic hazard assessments confirm that Iraq remains vulnerable to future earthquakes and that updated hazard studies are necessary to support safe engineering practice, particularly for sites underlain by loose, saturated sands that are susceptible to strength loss during shaking [12,13].

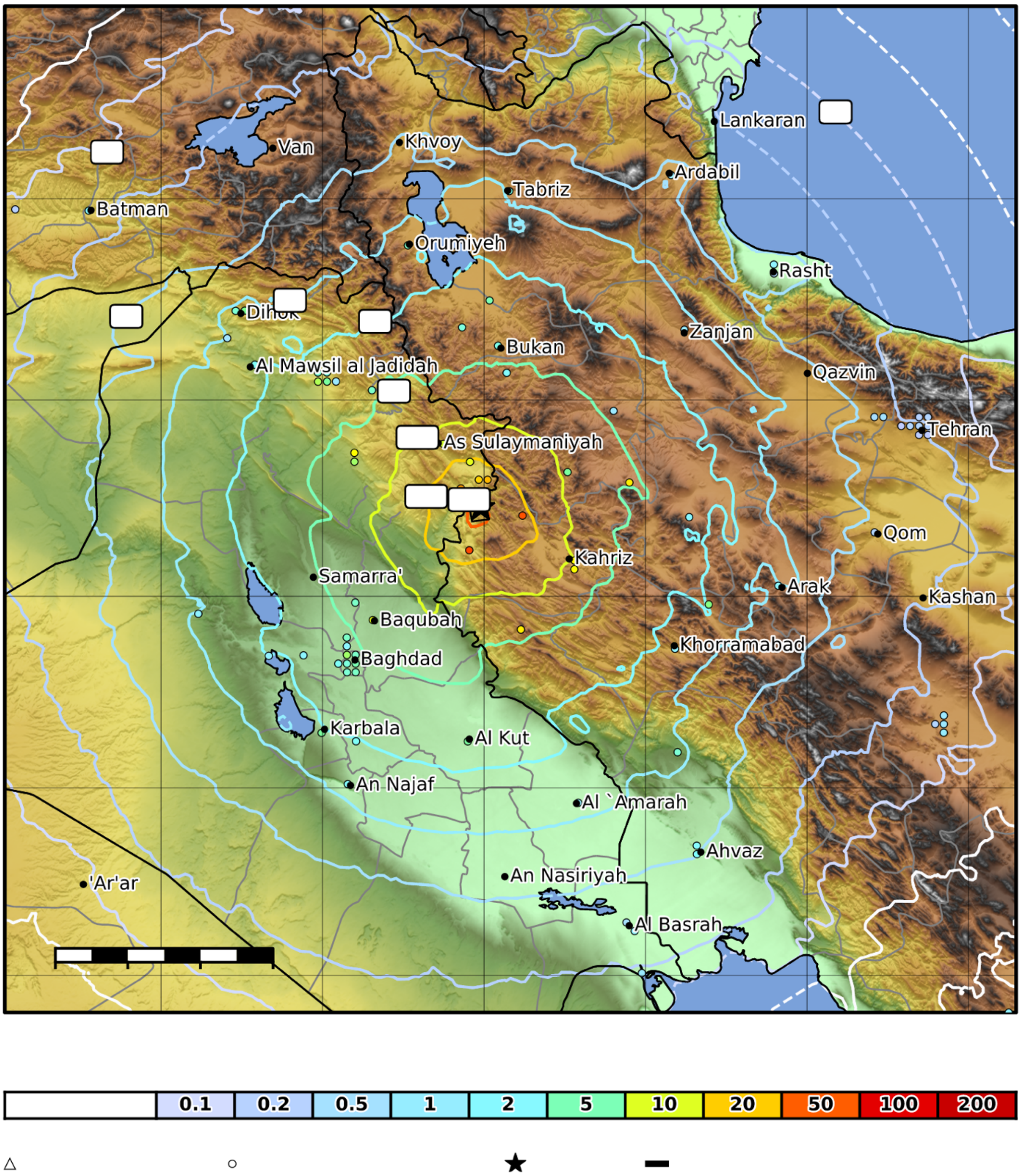

Figure 1. Seismological Map of the 2017 Halabja Earthquake (Source: USGS)

2.3 Halabja 2017 Earthquake and Regional Seismic Hazard

During 2017–2018, Iraq and the surrounding border region experienced elevated seismic activity, with the most significant event being the 12 November 2017 earthquake (Mw 7.3) located approximately 29 km south of Halabja near the Iran–Iraq border [16]. This mainshock was followed by numerous aftershocks and moderate events recorded by local and regional observatories, highlighting the continued seismic threat along the Iraq–Iran frontier. In the present work, the local Halabja 2017 acceleration time history (Fig. 1) is adopted as the input ground motion for dynamic analyses; the raw record was processed and plotted following the accelerogram reported in Abbas and Al-hadidi [14], while the event parameters correspond to the USGS documentation [16]. Field observations during major regional earthquakes indicate that saturated sandy deposits may undergo liquefaction, leading to loss of strength, sand boils, and differential settlement that can cause tilting, cracking, or even collapse of structures [12]. Therefore, strengthening of the superstructure alone may be insufficient if the foundation–soil system is not adequately accounted for. Against this backdrop, this study assesses the seismic behavior of the seven-story parking garage originally supported on bearing piles by comparing its response under recent ground motions and evaluating alternative raft foundation strategies, thereby addressing the need for focused investigation of earthquake effects on Iraqi foundation soils.

Table 1. Historical Seismic Events in Iraq Over the Last 100 Years [12]

Event No.	Year	Magnitude (Richter scale)	Remarks
1	1917	-	Earthquake hit Baghdad
2	1946	-	Severe earthquake hit Baghdad
3	1960	6.0 to 6.7	Earthquakes hit Halabja city northeast of Baghdad and caused severe damages
4	1967	6.1	Earthquakes hit 100 km south of Halabja city, northeast of Baghdad.
5	2013	5.6 and 5.8	Two Earthquakes hit 60 km south of Halabja city, northeast of Baghdad
6	2017	7.3	Series of earthquakes with maximum magnitude of 7.3 hit 30 km south of Halabja city, northeast of Baghdad, Iraq
7	2018	4.0 to 4.5	Series of earthquakes hit northeast Baghdad, Iraq

3. Method

3.1 Structural Model Characteristics

The structural model is defined by plan dimensions of (85 × 50) m in the X and Y directions respectively as shown in Fig. 2. The total height of the building is 26 m. A circular vehicular ramp is integrated along the Y-axis, with a radius of 14 m. The structural plan layout is shown in Fig. 2.

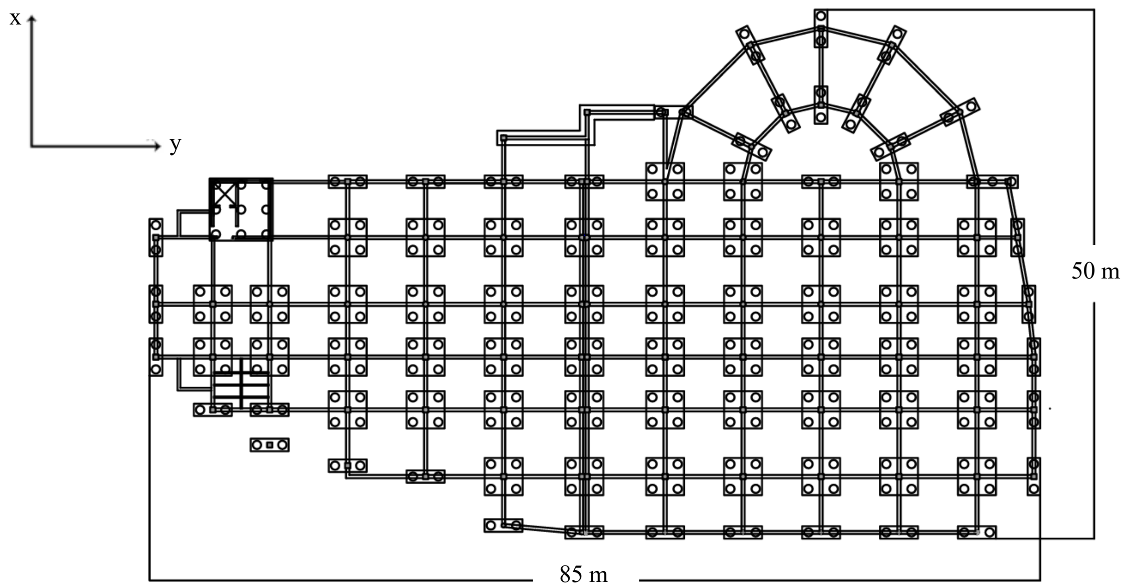

Figure 2. Structural Plan of the Studied Building

The structural numerical modeling using finite element method via PLAXIS 3D is shown in Fig. 3. The configurations of the foundation as a fixed base, columns and slabs are shown in this figure. The mesh element has been used for the slabs and raft and/or pile caps foundations, and the beam elements have been used for simulating the columns of the structure.

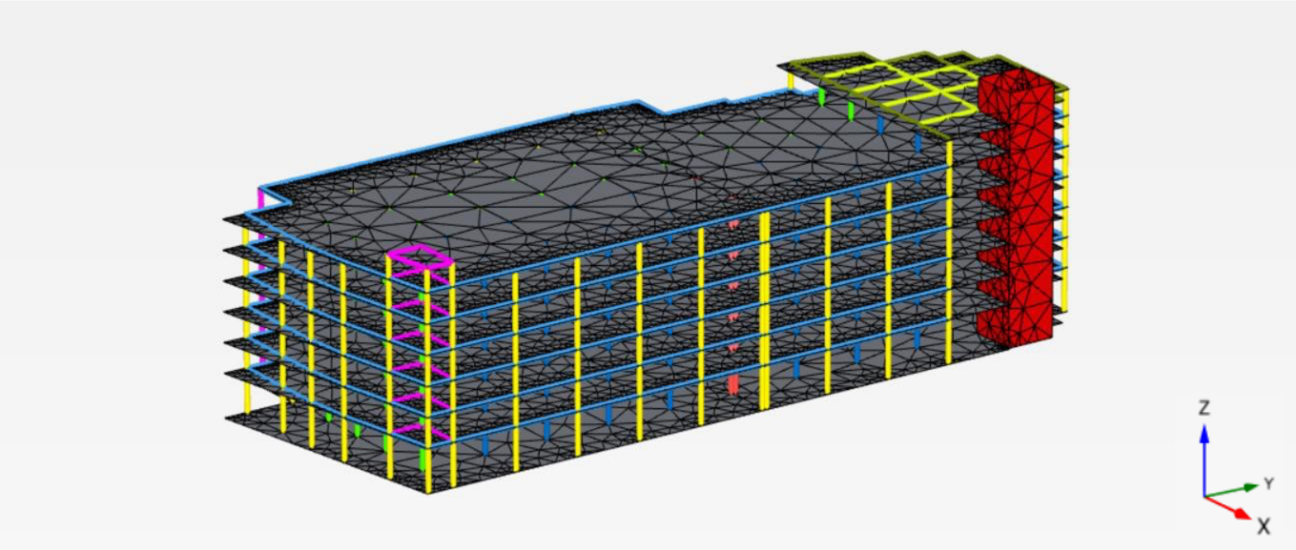

Figure 3. Three-Dimensional Finite-Element Model of the Structure in PLAXIS 3D

The modulus of elasticity (E) of the reinforced concrete material is 25000 MPa, with damping of 3% and the thickness of the floor slab is 250 mm. The cross-sectional dimensions of columns and shear walls were selected to satisfy a design reinforcement ratio limit of 2%, as listed in Table 2.

Table 2. Column and Shear Wall Sections

Symbol	Cross Section (mm)
C1	Ø 600
C2	600 × 600
C3	500 × 500
C4	400 × 400
C5	Ø 400
C6	500 × 500
C7	Ø 500
SW1	200*4700
SW2	200*3250
SW3	200*3250
SW4	200*3250
SW5	200*3250
SW6	200*3250
SW7	200*2800

3.2 Soil Model Characteristics

The dimensions of the soil domain were selected to provide a sufficiently large and conservative model space in all directions for the dynamic SSI analysis. In the present study, free-field boundaries were assigned along the lateral sides of the model, while a compliant base was used at the bottom boundary, in accordance with the PLAXIS approach recommended for earthquake analyses in which the dynamic input is applied at the model boundaries. The adopted domain dimensions were 470 m in the global X-direction, 430 m in the global Y-direction, and 80 m in depth. The slightly larger extent in the X-direction was intentionally selected because the earthquake excitation was applied along this direction. Extending the domain in the direction of input motion helps reduce artificial wave reflections from the boundaries and provides a more realistic representation of seismic-wave propagation through the supporting soil. Overall, the adopted boundary dimensions were considered sufficiently large and conservative in the X-, Y-, and Z-directions to simulate semi-infinite soil conditions and to improve the reliability of the computed structural response.

The Hardening Soil with small-strain stiffness (HS-small) constitutive model was used to represent the soil types in our study area. This advanced soil model enables the capture of small-strain stiffness degradation and nonlinear hysteretic behavior. The properties of the soils are listed in Table 3.

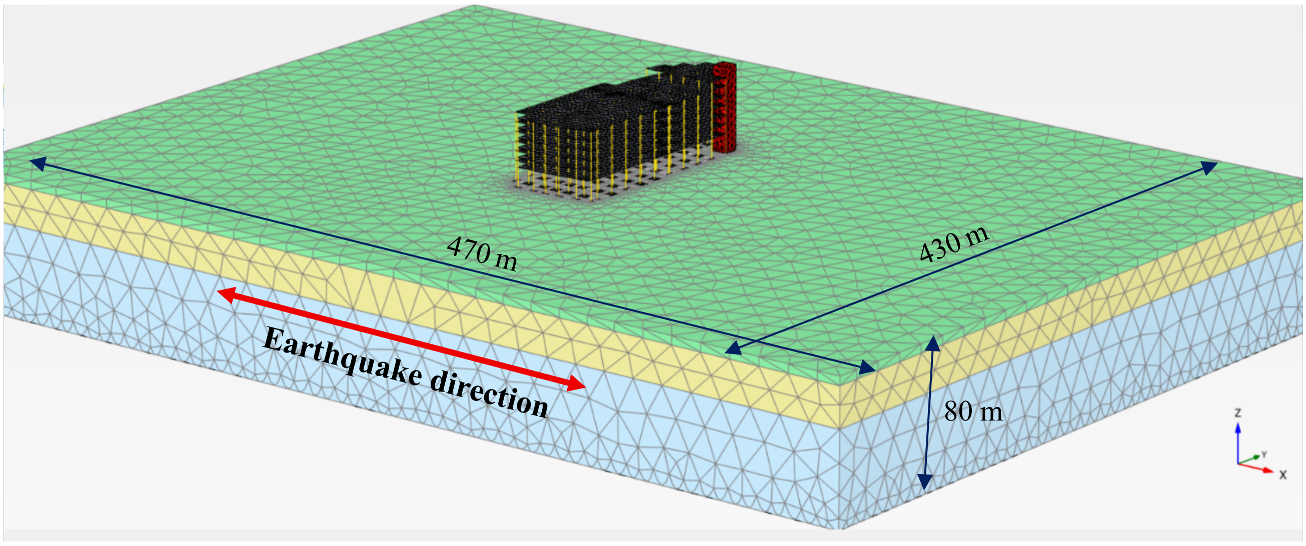

Figure 4. Three-Dimensional Model of the Soil Layers Coupled With the Structure

Table 3. Parameters of Site Soil Layers

Parameter	Units	First Layer (Fill)	Second Layer (Silty Clay)	Third Layer (Sand)	Fourth Layer (Hard Clay)
Thickness	[m]	2	2.6	11.8	63
γ_{unsat}	[kN/m³]	15	16	15	17
γ_{sat}	[kN/m³]	19	20	19.2	20.5
E_{50}^{ref}	[kN/m²]	30000	50000	60000	80000
$E_{\text{oed}}^{\text{ref}}$	[kN/m²]	40000	40000	50000	90000
$E_{\text{ur}}^{\text{ref}}$	[kN/m²]	80000	10000	110000	140000
m	[---]	0.5	0.5	0.5	0.5

Parameter	Units	First Layer (Fill)	Second Layer (Silty Clay)	Third Layer (Sand)	Fourth Layer (Hard Clay)
c	[kN/m²]	20	20	0.3	26
ϕ	[°]	8	8	34	2
ψ	[°]	2	2	0	5
ν_{ur}	[---]	0.2	0.2	0.2	0.2
G_0^{ref}	[kN/m²]	80000	100000	120000	160000
$\gamma_{0.7}$	[---]	0.002	0.02	0.017	0.02
Rayleigh α	[---]	0.0005	0.0005	0.0005	0.0005
Rayleigh β	[---]	0.005	0.005	0.005	0.005

The variation of the normalized shear modulus with cyclic shear strain was also considered to describe the strain-dependent stiffness degradation of the soil during dynamic loading. The relationships between G/G_{max} and cyclic shear strain for the soft soil and the actual site soil are presented in Fig. 5 (a) and Fig. 5 (b), respectively. These curves show the reduction in shear stiffness with increasing cyclic shear strain, which is important for representing the nonlinear dynamic response of the soil in the soil–structure interaction analysis.

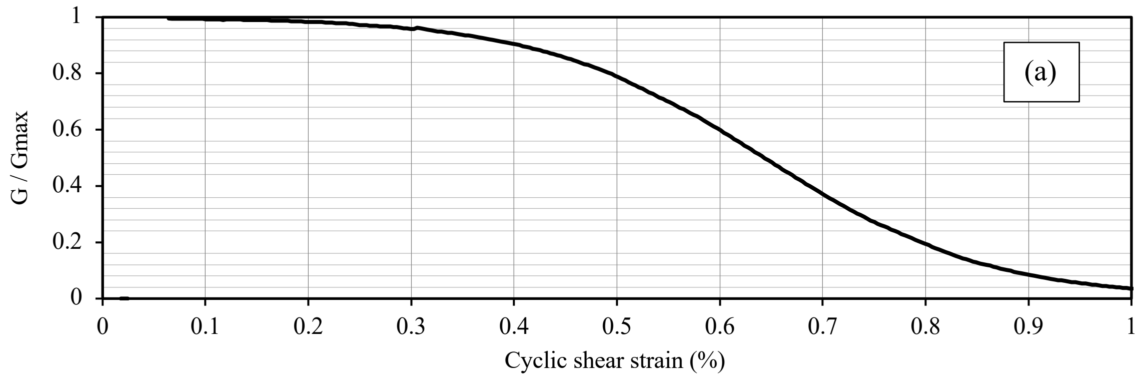

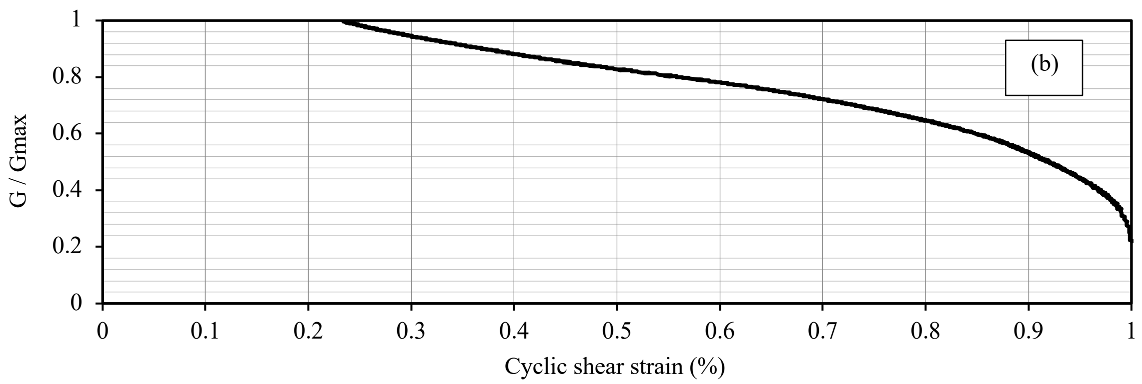

Figure 5. Relationships Between Normalized Shear Modulus (G/Gmax) and Cyclic Shear Strain for: (a) Soft Soil and (b) Site Soil

3.3 Static and Dynamic Loads

For the static load, according to ASCE 7-10 [15], the parking deck and roof are assigned a uniform live load of 2.4 kN/m², with no partition load assumed. In addition, concentrated wheel loads of 40 kN per wheel contact have been applied at regular intervals and in numbers corresponding to typical daily parking-garage occupancy. For the fixed-base reference case, the column bases were modeled as fully restrained; the SSI cases used the corresponding pile or raft foundation–soil system. The concrete compressive strength in walls and frame members is taken as 55 MPa. For dynamic loading, the Halabja 2017 earthquake acceleration record was applied at the base of the soil domain as a time series without scaling or modification as shown in Fig. 6.

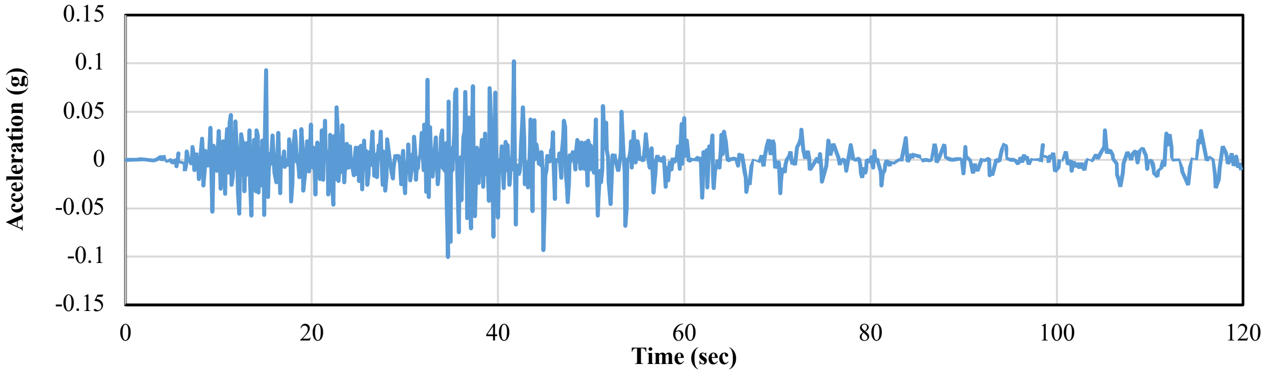

Figure 6. Halabja Earthquake Acceleration Record

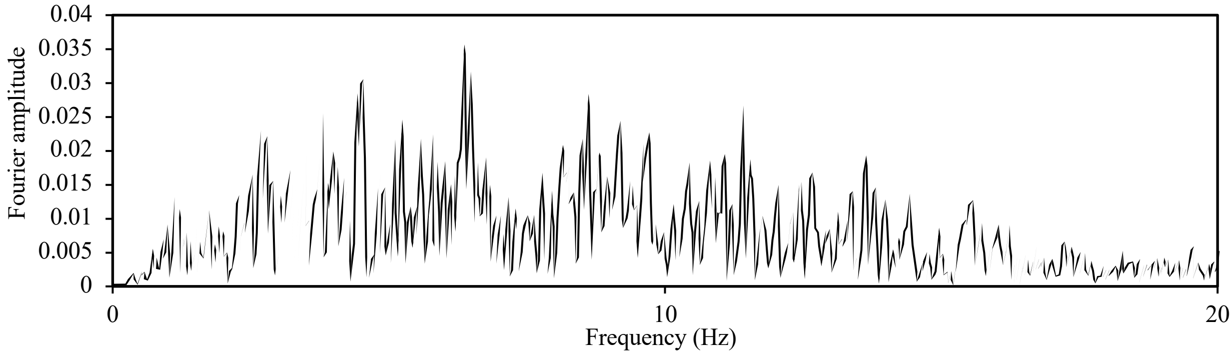

Figure 7. Fourier Spectrum of the Halabja 2017 Record

3.4 Design Response Spectrum

To define the seismic demand at the site quantitatively, the earthquake ground motion function is characterized by the mapped spectral response acceleration parameters Ss (at 0.2 s period) and S1 (at 1.0 s period), together with the peak ground acceleration (PGA). According to the current Iraqi seismic code, which follows the ASCE 7-10 methodology with locally mapped parameters referenced to Site Class B (rock), the values assigned to Halabja city are Ss = 2.16 g and S1 = 0.86 g, with a corresponding code-level PGA of 0.576 g [12, 18]. These values, among the highest in Iraq, reflect the proximity of the site to the active Zagros convergent boundary and are summarized in Table 4.

Table 4. Design Response Spectrum Parameters for Halabja (Ss = 2.16 g, S1 = 0.86 g)

Site Class	SDS (g)	SD1 (g)	PGA (g)
B (Rock)	1.44	0.57	0.576
D (Stiff soil)	1.44	1.15	0.576
E (Soft soil)	1.30	1.61	0.518

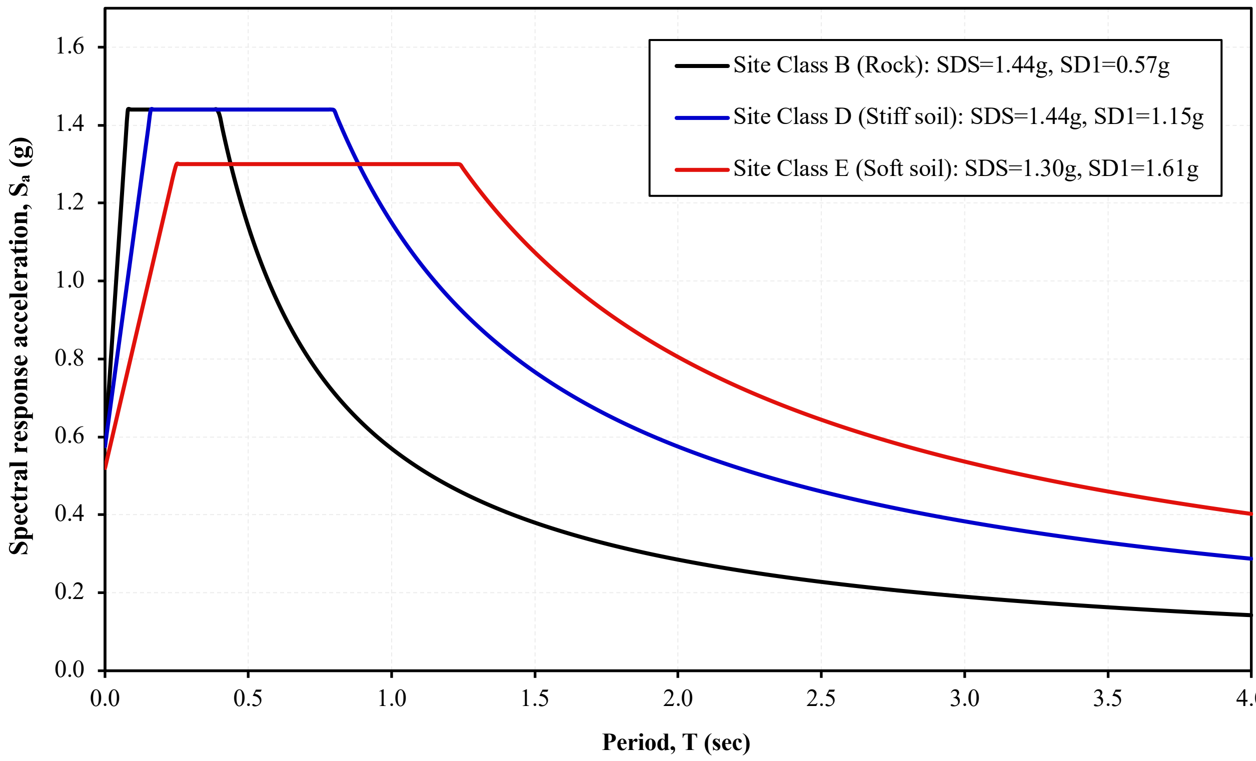

Figure 8. Design Response Spectra for Halabja (Ss = 2.16 g, S1 = 0.86 g, PGA = 0.576 g)

3.5 Implementation of Soil–Structure Interaction

A fully integrated finite-element analysis was conducted to capture the interaction between the superstructure, foundation, surrounding soil, and seismic excitation. This was achieved in PLAXIS 3D by selecting a fully coupled dynamic analysis that applies consistent treatment to both soil and structural behavior. Contact between the raft foundation and soil was modeled using zero-thickness interface elements, allowing slip and separation according to defined stiffness and strength parameters, with an interface shear-strength reduction factor Rinter = 0.9. Free-field boundaries were applied laterally, and a compliant base was implemented to simulate a semi-infinite soil medium. The 2017 Halabja acceleration time history was applied at the model base as the dynamic input record. Time-domain simulations provided key seismic response indicators such as lateral displacement, inter-story drift, fundamental period, and base shear, while fully capturing the effects of soil–structure interaction.

3.6 Numerical Modeling Procedure

To implement the numerical simulations via Plaxis 3D, there are subsequent stages that must be done step by step as follows:

1. Define the geometry of the system, including the mid-rise building and the soil domain.
2. Define the material properties of concrete and soil.
3. Assign the mechanical behavior of the soil and structural elements, including elasticity, plasticity, and damping.
4. Integrate the structure and soil domain within the finite-element model.
5. Apply the loads and appropriate boundary conditions.
6. Define the foundation–soil interaction through the interface connections between the raft and the soil.
7. Carry out the parametric dynamic analyses using the implicit solution approach and extract the soil–structure interaction response quantities.
8. Compare the SSI response for the idealized soft-soil profile and the actual site-specific soil

profile in the stated direction of excitation.

4. Results and Discussion

4.1 Lateral Displacement

The displacements, inter-story drift ratios, time periods, and base shear values obtained for the two structural models under soft soil and site soil conditions are presented in Figs. 9–20. The displacement results are shown in Figs. 9–12. The minimum displacement value was obtained from the 7-story fixed-base model on site soil, which was 6.5 cm, whereas the maximum displacement value was obtained from the 14-story model on soft soil with a raft foundation size of 1.1B, which reached 26.5 cm. In general, the displacement values increased with increasing building height and with stronger soil–structure interaction effects. For both the 7-story and 14-story buildings, the displacement became larger as the raft foundation size decreased from 2B to 1.1B. In contrast, increasing the raft size reduced the displacement response and brought the results closer to those of the fixed-base case. This trend was more pronounced for the site soil model, where the 7-story building with a raft size of 2B gave a displacement of 6.8 cm compared with 6.5 cm for the fixed-base case, indicating a very close response.

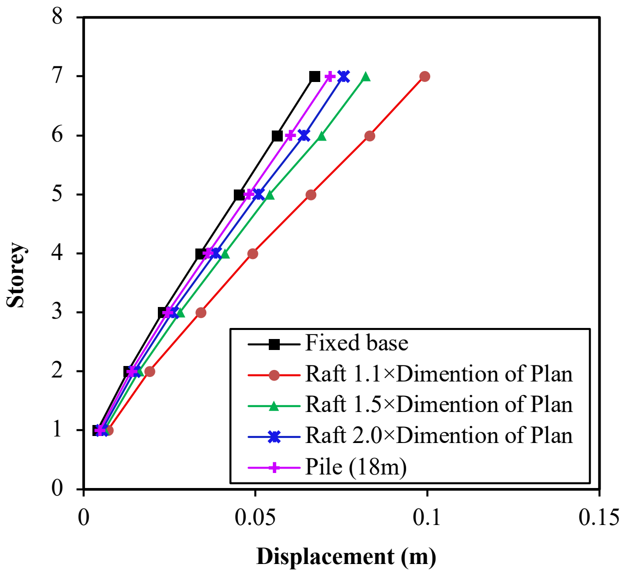

Figure 9. Soft-Soil Displacement (7-Storey)

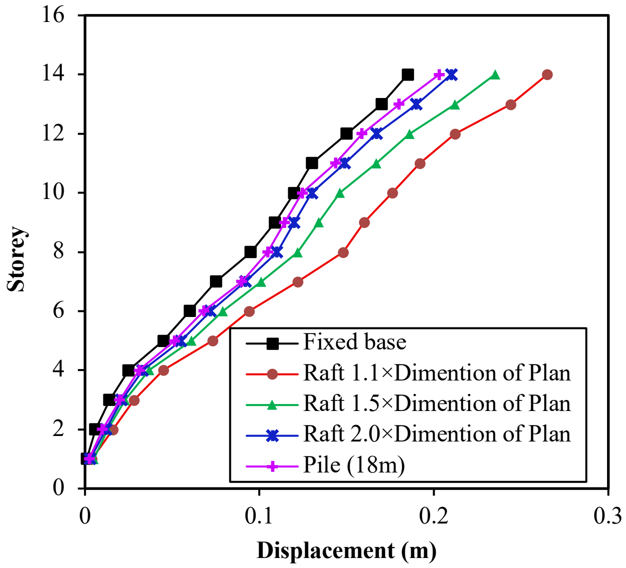

Figure 10. Soft-Soil Displacement (14-Storey)

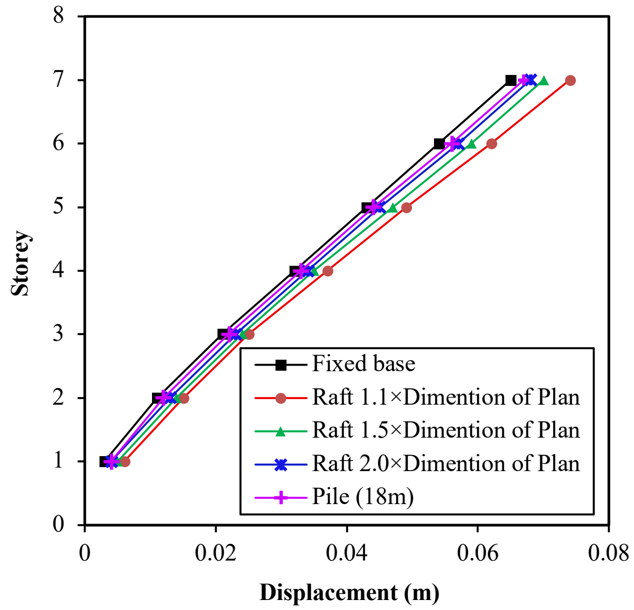

Figure 11. Site-Soil Displacement (7-Storey)

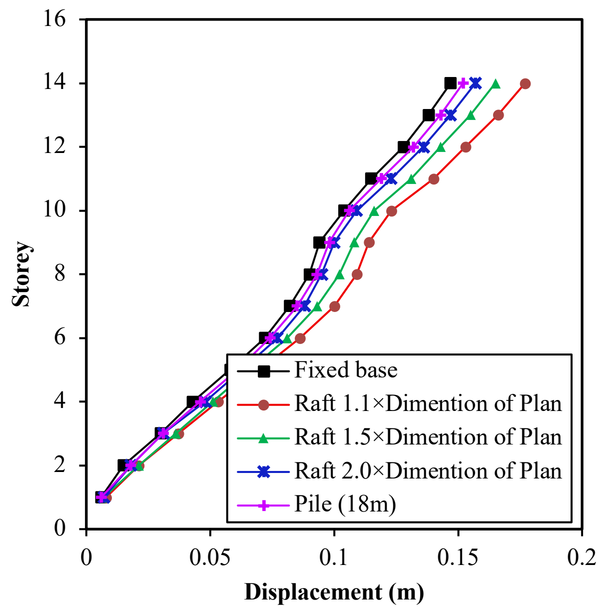

Figure 12. Site-Soil Displacement (14-Storey)

4.2 Inter-Storey Drift Ratio

The inter-story drift ratios are presented in Figs. 13–16. The minimum drift ratio was recorded for the 7-story fixed-base model on site soil, with a value of 0.179%, while the maximum drift ratio was observed for the 14-story model on soft soil with a raft foundation size of 1.1B, where it reached 1.609%. Similar to the displacement trend, the drift ratios increased as the foundation system became more flexible and as the soil condition became softer. For both structural heights, decreasing the raft size from 2B to 1.1B increased the drift ratio noticeably, whereas increasing the raft size reduced the drift and caused the values to approach those of the fixed-base model. For example, in the 7-story model on site soil, the drift ratio increased from 0.179% in the fixed-base case to 0.223% at 1.1B, while the corresponding value at 2B was only 0.192%. In the 14-story model, the same tendency was observed, with much larger drift values under soft soil than under site soil.

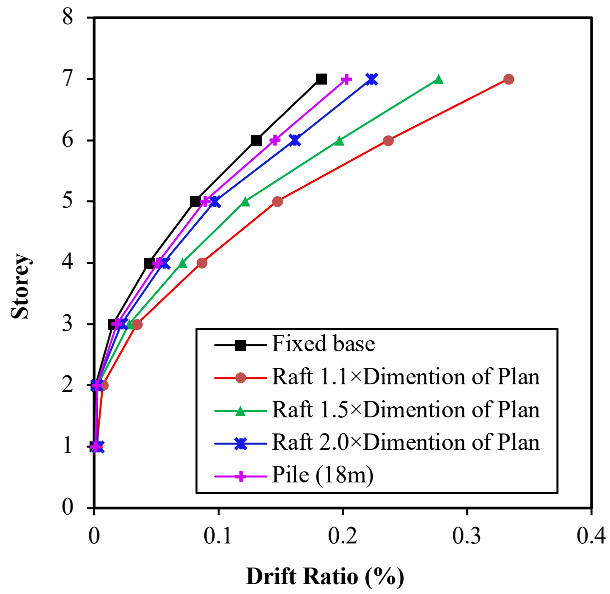

Figure 13. Soft-Soil Inter-Storey Drift Ratio (7-Storey)

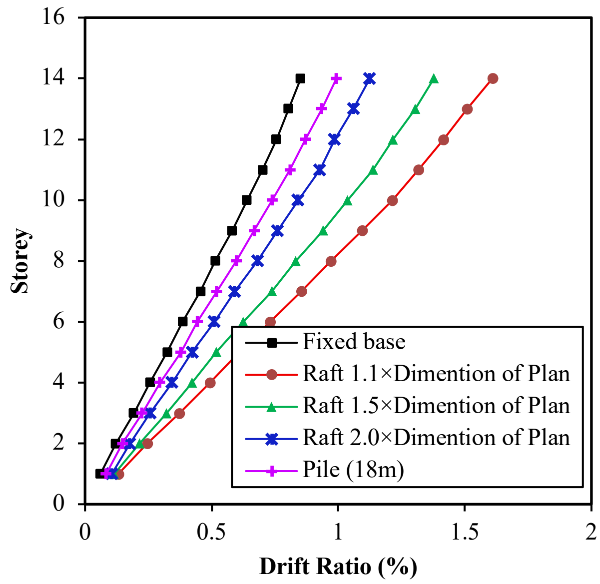

Figure 14. Soft-Soil Inter-Storey Drift Ratio (14-Storey)

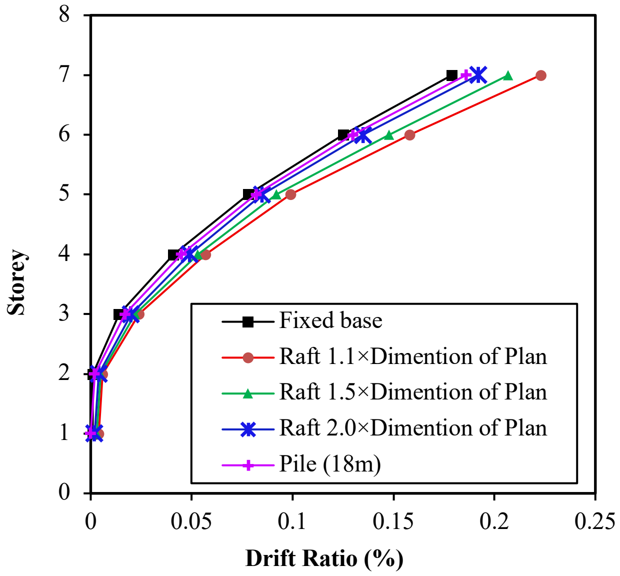

Figure 15. Site-Soil Inter-Storey Drift Ratio (7-Storey)

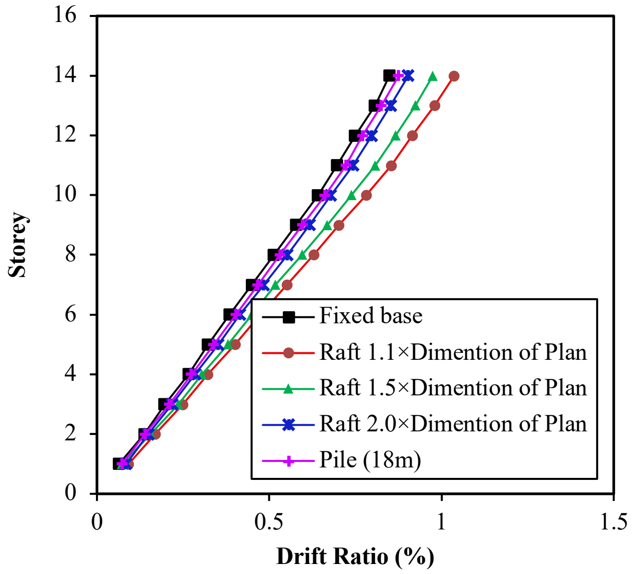

Figure 16. Site-Soil Inter-Storey Drift Ratio (14-Storey)

4.3 Fundamental Period

The time period values are illustrated in Figs. 17 and 18. The minimum time period was obtained from the 7-story fixed-base model on site soil, with a value of 0.75 s, whereas the maximum time period was obtained from the 14-story model on soft soil with a raft foundation size of 1.1B, which reached 2.46 s. The results indicate that the structural period increased with increasing soil flexibility and decreasing raft size, reflecting the reduction in the overall stiffness of the soil–foundation–structure system. For the 7-story model, the time period increased from 1.28 s in the fixed-base case on soft soil to 1.97 s at 1.1B, while for the 14-story model it increased from 2.21 s to 2.46 s for the same cases. Under site soil conditions, the time periods were generally smaller than those of the corresponding soft soil cases and remained closer to the fixed-base response, especially when the raft size was 2B.

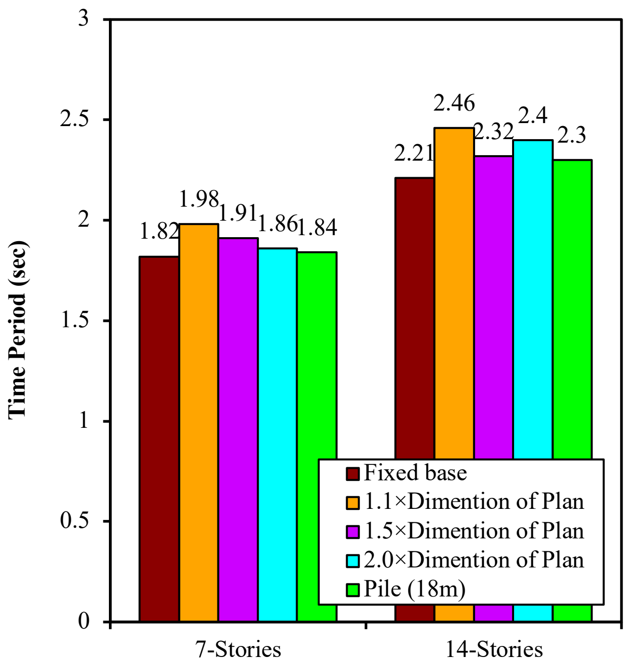

Figure 17. Fundamental Period (Soft Soil)

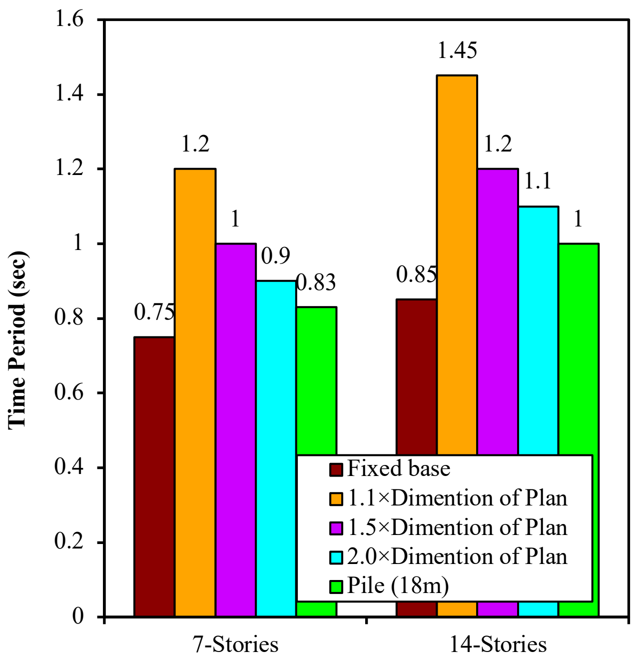

Figure 18. Fundamental Period (Site Soil)

4.4 Base Shear

The base shear values are shown in Figs. 19 and 20. The minimum base shear value was obtained from the 7-story building with a raft foundation size of 1.1B, which was 12,024,998 N, whereas the maximum base shear value was obtained from the 14-story fixed-base model, which reached 18,945,819 N. In both structural models, the base shear increased as the raft size increased and approached the fixed-base case when the raft foundation size reached 2B. For instance, in the 7-story model, the base shear increased from 12,024,998 N at 1.1B to 14,417,247 N at 2B, compared with 15,156,656 N for the fixed-base case. Likewise, in the 14-story model, the base shear increased from 15,031,248 N at 1.1B to 17,817,133 N at 2B, compared with 18,945,819 N for the fixed-base case. The pile-supported case generally gave intermediate values between the more flexible raft systems and the fixed-base model.

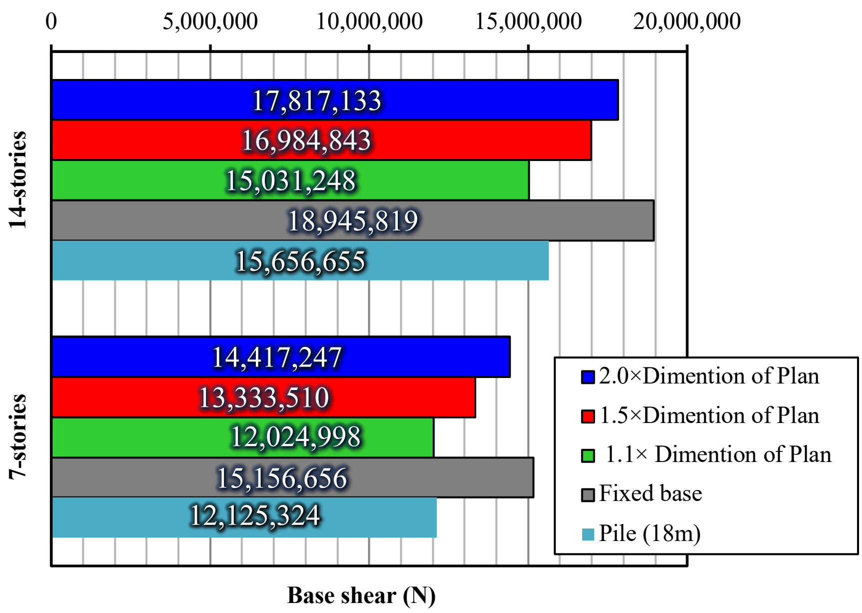

Figure 19. Base Shear (Site Soil)

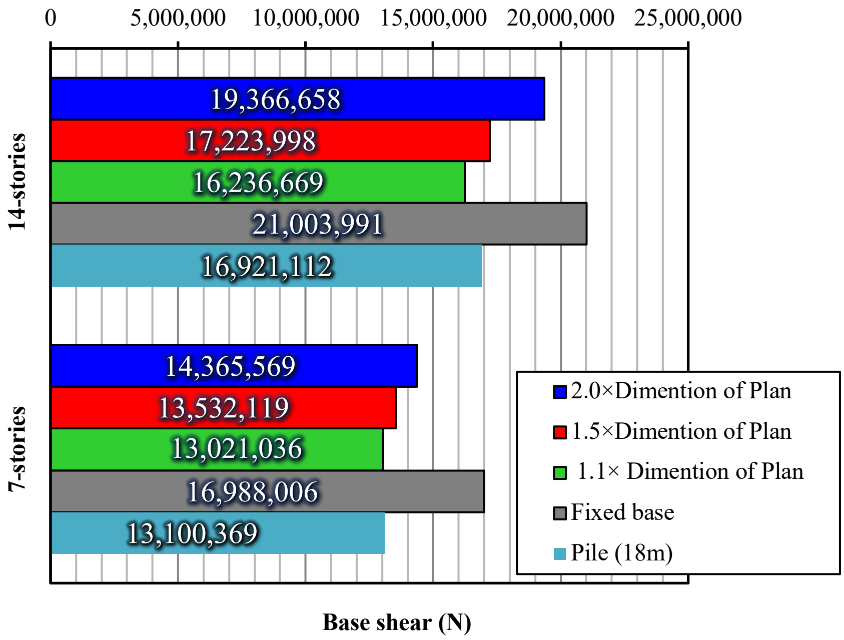

Figure 20. Base Shear (Soft Soil)

4.5 Discussion

1. **Displacement and drift amplification.** Moving from the fixed-base case to pile-supported, smaller rafts, and finally the idealized soft-soil profile progressively reduces the lateral and rotational stiffness of the soil-foundation-structure system. Since period varies inversely with the square root of system stiffness, this lengthens the fundamental period (Figs. 17-18), consistent with Gazetas and Mylonakis [1] and Stewart et al. [2]. As the period approaches, and for the 14-story soft-soil cases exceeds, the input motion's corner period, spectral displacement demand grows. This explains why the largest displacement (26.5 cm) and drift (1.61%) occur for the 14-story building on soft soil with the smallest raft (1.1B), where the period lengthens most, to 2.46 s.
2. **Base shear.** Base shear depends on effective seismic mass times spectral acceleration at the (lengthened) period, not on displacement. Since the response spectra decays beyond their corner period, spectral acceleration falls as period lengthens. More flexible systems thus undergo larger displacement while attracting lower base shear (Figs. 19-20), a trade-off well established in the SSI literature [1,2,9].
3. **Role of raft size.** Enlarging the raft from 1.1B to 2B increases both translational and rotational (rocking) stiffness, but rotational stiffness scales roughly with the cube of raft dimension while translational stiffness scales only linearly. Suppressing rocking is therefore far more effective in restoring fixed-base behavior, explaining why 2B cases converge closely to fixed-base values (e.g., 7-story site-soil displacement of 6.8 cm at 2B versus 6.5 cm fixed-base, within 5%).
4. **Role of soil type.** The site soil, with its medium-dense sand (φ = 34°) and thick hard-clay layer, provides greater confinement and stiffness than the idealized soft profile, so SSI effects are consistently smaller for the same foundation configuration. Soil condition and foundation stiffness thus act as compounding variables in controlling SSI severity.
5. **Role of building height.** The 14-story model amplifies every SSI effect relative to the 7-story model under identical soil-foundation conditions, since a taller structure's already-longer fixed-base period lengthens further into the range of sustained spectral demand, consistent with Gazetas and Mylonakis [1]. This is why the critical combination (14 stories, soft soil, 1.1B raft) stacks all three amplifying factors together.

6. **Piles as an intermediate case.** The pile-supported foundation (18 m length) consistently gave displacement, drift, period, and base-shear values between the flexible-raft and fixed-base cases, since deep foundations transfer load past near-surface soft layers into stiffer strata at depth, partially restoring fixity that a shallow raft cannot achieve.

5. Conclusion

- The effects of soil–structure interaction (SSI), fixed-base assumptions, and different foundation systems, including pile foundations and raft foundations of different sizes, were investigated for 7-story and 14-story reinforced concrete buildings subjected to seismic loading.
- The results showed that lateral displacement, inter-story drift, and fundamental period generally increased with increasing soil flexibility and decreasing foundation stiffness, whereas base shear decreased compared with the fixed-base condition.
- The most critical response was observed in the 14-story building resting on soft soil with the smallest raft foundation size (1.1B), where the maximum values of displacement, drift ratio, and time period were recorded.
- The responses of the site soil cases were generally closer to those of the fixed-base model, especially when the raft foundation size reached 2B.
- The pile-supported foundation system produced intermediate results between the fixed-base case and the more flexible raft foundation cases under both soil conditions.
- Increasing the raft foundation size improved the seismic behaviour of the studied buildings by reducing displacement, inter-story drift, and time period, while increasing base shear toward the fixed-base response.
- Overall, the study confirms that both soil condition and foundation configuration have a significant influence on the seismic performance of mid-rise reinforced concrete buildings and therefore should be explicitly considered in seismic analysis and design.

Declaration of Competing Interest

The authors declare that there are no conflicts of interest regarding the publication of this manuscript.

Funding Information

No funding was received from any financial organization to conduct this research.

Author Contributions

All authors proposed the research problem. In addition, author Issa Al-Musawi conducted numerical modeling, performed numerical analyses, interpreted the results, and prepared the original manuscript. Author Asad H. Aldefae provided the drawings and the geotechnical and soil data. Author Karrar Al-Lami provided structural and seismic data. Author K.I.M Ismail verified the results and reviewed and refined the manuscript. All authors discussed the results and approved the final version of this paper.

Notation List

Abbreviations / Symbols	Meaning
SSI	Soil–Structure Interaction
RC	Reinforced Concrete
FEM	Finite Element Method
HS-small	Hardening Soil model with small-strain stiffness
Mw	Moment magnitude
PGA	Peak Ground Acceleration
Ss	Mapped spectral response acceleration at a period of 0.2 s

Abbreviations / Symbols	Meaning
S1	Mapped spectral response acceleration at a period of 1.0 s
SDS	Design spectral response acceleration at short periods
SD1	Design spectral response acceleration at a period of 1.0 s
B	Reference building width (50 m) used to define raft plan dimensions
E	Modulus of elasticity
γunsat	Unsaturated unit weight of soil
γsat	Saturated unit weight of soil
E50ref	Reference secant stiffness in drained triaxial loading
Eoedref	Reference tangent stiffness for primary oedometer loading
Eurref	Reference unloading/reloading stiffness
m	Stress-dependency exponent in the HS-small model
c	Soil cohesion
φ	Soil friction angle
ψ	Soil dilatancy angle
νur	Poisson's ratio for unloading/reloading
G0ref	Reference small-strain shear modulus
γ0.7	Threshold shear-strain parameter used in the HS-small model
α	Rayleigh mass-proportional damping coefficient
β	Rayleigh stiffness-proportional damping coefficient
Rinter	Interface strength-reduction factor
G/Gmax	Normalized shear modulus

References

[1] G. Gazetas and G. Mylonakis, "Seismic soil-structure interaction: new evidence and emerging issues," Geotech. Spec. Publ., no. 75 II, pp. 1119–1174, Dec. 1998.

[2] J. P. Stewart, R. B. Seed, and G. L. Fenves, "Seismic soil-structure interaction in buildings. II: Empirical findings," J. Geotech. Geoenviron. Eng., vol. 125, no. 1, pp. 38–48, Jan. 1999, doi: 10.1061/(ASCE)1090-0241(1999)125:1(38).

[3] T. Balendra and A. C. Heidebrecht, "Influence of different sites on seismic base shear of buildings," Earthquake Eng. Struct. Dyn., vol. 14, no. 4, pp. 623–642, Jul. 1986, doi: 10.1002/eqe.4290140410.

[4] M. A. Ghannad, A. Amiri, and S. F. Ghahari, "Effects of soil-structure interaction on response of structures subjected to near-fault earthquake records," AIP Conf. Proc., vol. 1020, no. 1, pp. 642–649, Jul. 2008, doi: 10.1063/1.2963896.

[5] J. Rajasankar, N. R. Iyer, B. Y. Swamy, N. Gopalakrishnan, and P. Chellapandi, "SSI analysis of a massive concrete structure based on a novel convolution/deconvolution technique," Sadhana, vol. 32, no. 3, pp. 215–234, Jun. 2007, doi: 10.1007/s12046-007-0019-5.

[6] B. Alavi and H. Krawinkler, "Behavior of moment-resisting frame structures subjected to near-fault ground motions," Earthq. Eng. Struct. Dyn., vol. 33, no. 6, pp. 687–706, May 2004, doi: 10.1002/eqe.369.

[7] M. A. Adam, O. A. Kamal, and M. El-Hoseny, "Variation of seismic response of mid-rise RC buildings due to soil structure interaction effects," Int. J. Civ. Eng. Technol. (IJCIET), vol. 7, no. 1, pp. 220–240, 2016.

[8] K. Galal and M. Naimi, "Effect of soil conditions on the response of reinforced concrete tall structures to near-fault earthquakes," Struct. Des. Tall Spec. Build., vol. 17, no. 3, pp. 541–562, Sep. 2008, doi: 10.1002/tal.365.

[9] J. P. Stewart, R. B. Seed, and G. L. Fenves, Empirical Evaluation of Inertial Soil-Structure Interaction Effects, Report No. PEER-98/07, Pacific Earthquake Engineering Research Center (PEER), University of California, Berkeley, Nov. 1998.

[10] S. Ismail, F. Kaddah, and W. Raphael, "Assessing the Dynamic Behaviour of Midrise Frame Structures Sitting on Silty Sandy Soil," Open Civ. Eng. J., vol. 14, pp. 262–288, 2020, doi: 10.2174/1874149502014010262.

[11] S. Carbonari, F. Dezi, and G. Leoni, "Nonlinear seismic behaviour of wall-frame dual systems accounting for soil–structure interaction," Earthq. Eng. Struct. Dyn., vol. 41, no. 12, pp. 1651–1672, Oct. 2012, doi: 10.1002/eqe.1195.

[12] A. J. Al-Taie and B. S. Albusoda, "Earthquake hazard on Iraqi soil: Halabjah earthquake as a case study," Geodesy and Geodynamics, vol. 10, no. 3, pp. 196–204, 2019, doi: 10.1016/j.geog.2019.03.004.

[13] M. S. Farman and A. I. Said, "Updated Probabilistic Seismic Hazard Assessment for Iraq/2018," Civil Eng. J., vol. 4, no. 7, pp. 1610–1628, 2018, doi: 10.28991/cej-0309199.

[14] H. Abbas and M. Th. Al-hadidi, "Effect of Halabjah Earthquake on Al-Wand Earth Dam: Numerical Analysis," E3S Web Conf., vol. 318, p. 01016, 2021, doi: 10.1051/e3sconf/202131801016.

[15] ASCE/SEI, Minimum Design Loads for Buildings and Other Structures, ASCE/SEI 7-10, American Society of Civil Engineers, 2010.

[16] U.S. Geological Survey, "M 7.3 - 29 km S of Halabjah, Iraq," USGS Earthquake Hazards Program, Event ID: us2000bmcg, 12 Nov. 2017.

[17] E. A. M. S. Al-Heety, "A complete and homogeneous magnitude earthquake catalogue of Iraq," Arabian J. Geosci., vol. 7, no. 11, pp. 4727–4732, 2014, doi: 10.1007/s12517-013-1131-y.

[18] Ministry of Construction and Housing, Central Organization for Standardization and Quality Control, Iraqi Seismic Code Requirements for Buildings (ISC-2017), Baghdad, Iraq, 2017.